Peering Through The Dust: Paschen-beta Indicators of Star Formation and Dust Attenuation

Scientific Category: Galaxies
Scientific Keywords: Emission Line Galaxies, Galaxy Evolution, Star Formation, Starburst Galaxies
Budget Size: Regular

Abstract

We propose a comprehensive archival survey of attenuation-insensitive Paschen-beta star formation rates and histories, resolved line maps, and dust attenuation estimates from existing 3D-HST G141 observations of ~400 low-redshift galaxies. This large sample is made possible only by the unique combination of near-IR sensitivity and high multiplexing of the HST G141 grism. The 3D-HST survey provides the ideal dataset, augmented by CANDELS multiwavelength photometry that is among the deepest in the sky, plus public catalogs of ground-based optical spectra and H-alpha line fluxes. However, this proposal represents an entirely different experiment than the science cases of the initial 3D-HST proposal. Our study is also an effective low-redshift pathfinder for JWST Paschen-line observations of high-redshift galaxy samples observed in the near future.

Investigators:

Investigators and Team Expertise are included in this preview for your team to review. These will not appear in the version of the proposal given to the TAC, to allow for a dual anonymous review.

	Investigator	Institution	Country
	Bren Backhaus	University of Connecticut	USA/CT
	Nikko J. Cleri	University of Connecticut	USA/CT
	Vicente Estrada-Carpenter	Texas A & M University	USA/TX
*	Dr. Chris Faesi	Max-Planck-Institut fur Astronomie, Heidelberg	DEU
	Prof. Steven L. Finkelstein	University of Texas at Austin	USA/TX
	Dr. Kristian Finlator	New Mexico State University	USA/NM
	Prof. Mauro Giavalisco	University of Massachusetts - Amherst	USA/MA
	Dr. Intae Jung	NASA Goddard Space Flight Center	USA/MD
	Dr. Jasleen Matharu	Texas A & M University	USA/TX
	Dr. Ivelina G Momcheva	Space Telescope Science Institute	USA/MD
	Dr. Desika Narayanan	University of Florida	USA/FL
	Dr. Casey Papovich	Texas A & M University	USA/TX
	Dr. Raymond Simons	Space Telescope Science Institute	USA/MD
	Prof. Jonathan R Trump	University of Connecticut	USA/CT
	Dr. Benjamin Weiner	University of Arizona	USA/AZ

Number of investigators: 15

* ESA investigators: 1

Team Expertise:

The PI and Co-I's have extensive experience designing, reducing, analyzing, and publishing HST G102 and G141 grism observations. As part of the CLEAR, 3D-HST, and CANDELS teams, the PI and Co-I's have published over 100 refereed papers using HST grism data. The graduate student PI will perform the bulk of the data reduction and science publications, supervised by the admin PI and other Co-I's.

Scientific Justification

Peering through the Dust: Paβ Indicators of Star Formation and Attenuation

The Paschen lines of hydrogen are "gold standard" indicators of recent star formation (Kennicutt & Evans 2012). Just like the more commonly used Balmer series, the Paschen lines are recombination lines that are highly sensitive to the ionizing ($E > 13.6$ eV) radiation of OB stars formed within the last <10 Myr, while remaining relatively insensitive to nuisance parameters like the temperature and density of the star-forming gas (Osterbrock 1989). Unlike the optical Balmer lines, however, the near-IR Paschen lines are far less affected by interstellar dust attenuation, so they can reveal otherwise hidden star-forming regions that are shrouded in gas and dust that is optically thick to Balmer emission. Paschen-line SFRs are especially important in highly attenuated and/or low-mass galaxies, where UV/optical SFR indicators tend to miss significant amounts of star formation.

We propose to measure Paβ star formation rates and histories, attenuation, and emission line maps from archival *HST* WFC3/G141 grism observations of ~400 emission-line galaxies at $z < 0.3$. Our proposed sample represents an order of magnitude increase over the samples of previous studies of Paschen-line star formation rates (Alonso-Herrero et al. 2006, Calzetti et al. 2007, Cleri et al. 2020). We will measure:

- **Star formation rates** (SFRs) and **star formation histories** (SFHs), combining the short-timescale (<10 Myr) Paβ SFRs with long-timescale (10-100 Myr) UV SFRs to measure bursty/smooth/declining star formation as a function of galaxy properties.
- **Dust attenuation** from combining Paβ with Hα fluxes measured from optical spectroscopy (available for ~150 galaxies in our sample), reaching deeper into dense star-forming clouds than previous attempts at Hα/Hβ studies of dust attenuation.
- **Resolved star formation maps**, well-measured in ~40 galaxies in our sample, to measure the inside-out / outside-in assembly of galaxies.

Our study uses archival 3D-HST grism observations in the five CANDELS fields (Momcheva et al. 2016). The CANDELS fields maximize the science return of our measured Paβ line fluxes by containing published catalogs of galaxy stellar masses (e.g. Barro et al. 2019), morphologies (van der Wel et al. 2012), and ground-based spectroscopy (e.g. Wirth et al. 2004). The 3D-HST and CANDELS projects were proposed entirely for studies of $z > 1$ galaxies, using the IR grisms for rest-frame optical spectroscopy. In contrast, our archival proposal focuses on rest-frame IR spectroscopy of $z < 0.3$ galaxies: a goal that is perfectly suited to the rich 3D-HST and CANDELS datasets and yet remains completely unexplored by these surveys.

We motivate this proposal to expand upon an initial study of 32 Paβ-emitting galaxies detected by *HST* grism observations in the CLEAR (*HST* Cycle 23: PI Papovich) survey (Cleri et al. 2020, Estrada-Carpenter et al. 2019 , Simons et al. 2021). An example G141 spectrum and Paβ line map from the CLEAR sample are shown in Figure 1. The 53 arcmin^2 CLEAR region includes 32 galaxies with Paβ emission detected at SNR>3 or objects with well-detected spectroscopic redshifts, leading to our estimate of ~400 galaxies over the larger

626 arcmin^2 of 3D-HST. As Figure 2 shows, the Paβ-detected galaxies span a broad range of rest-frame colors, A_v, and sizes among $M_\star > 10^7 M_\odot$ galaxies at $z < 0.3$, and we will use this diversity across the large sample of ∼400 galaxies to study SFR and dust attenuation across a broad range of galaxy properties.

Star Formation Rates and Histories Star formation is the principle operator and consequence of galaxy evolution. Hydrogen recombination lines are emitted by gas ionized by massive ($>15 M_\odot$) stars, and the short (<10 Myr) lifetimes of these massive stars means that hydrogen lines represent near-instantaneous SFRs. The most widely used SFR tracer is Hα, but Hα SFR estimates suffer significantly from (uncertain) dust attenuation in the line of sight. For example, Hα flux is halved at a modest attenuation of $A_V = 1$, and reduced by a factor of ∼10 in a dusty galaxy with $A_V = 3$, assuming a Calzetti et al. 2000 attenuation law. In contrast the Paβ hydrogen line is attenuated by only 25% at $A_V = 1$ and by half at $A_V = 3$. And like the Balmer lines, Paβ emission is only marginally sensitive to ISM conditions, changing by only ∼3% over 4 orders of magnitude in gas density and by ∼20% over a factor of 4 in temperature (Osterbrock 1989). **Paβ measures near-instantaneous SFRs with minimal effects from dust attenuation.** Following Kennicutt & Evans (2012) and the Case B ratio of Paβ/Hα (Osterbrock 1989), SFR is calculated from Paβ as:

$$\log(\dot{M}_\star)[M_\odot/\mathrm{yr}] = \log[L(\mathrm{Pa}\beta)] - 40.02 \quad (1)$$

The rich multiwavelength CANDELS dataset also provides SFR estimates from UV continuum emission (Skelton et al. 2014, Barro et al. 2019). The UV continuum emission measures the SFR averaged over 10-100 Myr, and so provides a longer-timescale comparison for the more recent (<10 Myr) SFR measured from Paβ, yet still has the issues of being highly sensitive to dust attenuation. The ratio of Paβ and UV SFRs, as shown for the CLEAR data in Figure 3, reveals the recent **star formation history** (SFH) of a galaxy, including bursty (high Paβ/UV), rapidly declining (low Paβ/UV), and smooth SFHs.

CANDELS also provides well-measured stellar populations (Barro et al. 2019) and morphologies (van der Wel et al. 2014). Figure 2 shows that the CLEAR sample of 32 Paβ-emitting galaxies is representative of the larger $z < 0.3$ population of $M_\star > 10^8 M_\odot$ galaxies in 3D-HST, in rest-frame color (i.e., stellar population), continuum dust attenuation, and morphology. These Paβ SFRs are especially important for highly dusty galaxies where UV/optical tracers are severely attenuated, and low-mass IR undetected galaxies (see center panel of Figure 2). This proposal represents an order of magnitude larger sample than the CLEAR sample and will measure **Paβ SFRs and SFHs for ∼400 galaxies across a broad range of stellar populations and morphologies.**

Dust Attenuation Because the recombination lines of hydrogen are insensitive to metallicity, temperature, and density, their ratios can be used to estimate attenuation in the light of sight. The most commonly used ratio is Hα/Hβ. But this rest-frame optical ratio only works for modestly attenuated galaxies, since it saturates at $A_V \sim 2$ (e.g. Groves et al. 2012). Even worse, Hα/Hβ attenuation measurements will entirely miss regions of the ISM that are optically thick to Hβ emission.

The Paβ/Hα ratio is a far more sensitive and reliable measure of dust attenuation, especially for moderately to extremely dusty galaxies. Figure 4 shows an example of the comparison between Paβ and Hα fluxes for 11 galaxies from the CLEAR sample with optical spectra from the Team Keck Treasury Redshift Survey (TKRS, Wirth et al. 2004). This small sample includes at least one very dusty galaxy for which the Hα/Hβ ratio misses much of the dust attenuation. About 1/3 of the CANDELS region includes public optical spectra of sufficient depth to detect Hα for almost every Paβ-detected galaxy (Hα/Paβ = 17.6 at $A_V = 0$): see the Analysis Plan for a description of these datasets. We will couple our proposed Paβ fluxes to these archival ground-based Hα fluxes to for reliable dust attenuation measurements in $\sim$150 galaxies. The CANDELS photometry additionally provides continuum attenuation estimates (Barro et al. 2019), enabling us to compare nebular and stellar attenuation across a broad range of Paβ/Hα attenuation and galaxy properties.

Value Added Products: Resolved Star Formation Maps The slitless G141 grism retains the $0\farcs12$ resolution of the *HST*/WFC3 detector, and so observed spectral features are spatially extended by the morphology of their emission. This means that our proposal will produced resolved Paβ emission-line maps in addition to the integrated Paβ fluxes. **Paβ line maps represent the spatial distribution of star formation and a spatially resolved view of galactic assembly that is largely unaffected by dust.**

Hα tends to have broader spatial profiles than the continuum emission, but it is not clear if this is due to inside-out galactic assembly (i.e., galaxy centers forming stars earlier) or simply the effects of higher dust attenuation in galaxy centers (Nelson et al. 2016). We will resolve this degeneracy with Paβ line maps, measuring resolved SFR profiles that are largely unaffected by dust.

We anticipate $\sim$40 galaxies ($\sim$10%) in the proposed sample to have individually detected Paβ line maps like the example shown in Figure 1. For the remainder of the $\sim$400 galaxies, we will stack spectra binned by stellar mass and morphology (similar to Nelson et al. 2016). Continuum-subtracted line maps will be produced by the `grizli` software (Brammer et al. 2019): see the Analysis Plan for details on this methodology.

Summary We propose a comprehensive survey of attenuation-insensitive Paβ star formation rates and histories, dust attenuation estimates, and spatially resolved emission-line maps from archival 3D-HST G141 observations of $\sim$400 low-redshift galaxies. This large sample is made possible only by the unique combination of near-IR sensitivity and high multiplexing of the *HST* G141 grism. The 3D-HST survey provides the ideal dataset, with supporting CANDELS multiwavelength photometry that is among the deepest in the sky, plus public catalogs of ground-based optical spectra and Hα line fluxes. Yet this proposal represents an entirely different experiment than the science cases of the initial 3D-HST proposal, just as the *HST* archive program is intended. Finally, it is worth noting that the *JWST* spectrographs are similarly well-equipped for Paschen-line observations for an even larger sample of galaxies to $z < 3$. This makes our study a beneficial low-redshift preparation for *JWST* Paschen-line observations of even larger galaxy samples observed in the near future.

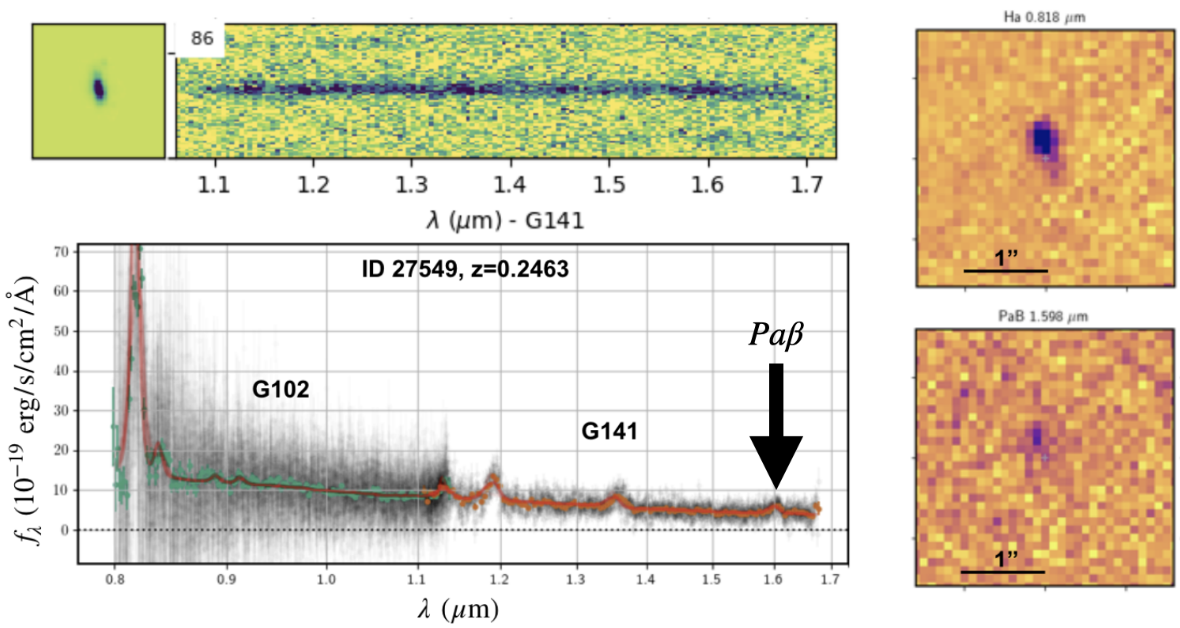

Figure 1: Direct F140W image (*top left*), observed-frame two-dimensional G141 spectrum (*top center*), observed-frame one-dimensional G102 and G141 spectra extracted with `grizli` (*bottom left*), and Hα and Paβ emission-line maps (*right*) for a galaxy in the CLEAR study. The Paβ line is indicated by the black arrow. **Our study will include ∼400 Paβ-emitting galaxies**, including ∼40 detections like this example with integrated Paβ SNR>10 and spatially resolved line maps.

Analysis Plan

We propose to use archival WFC3 G141 grism data in the five 3D-HST fields (Momcheva et al. 2016). Our Paβ science goals are entirely different from both the initial 3D-HST proposal and from all published 3D-HST work to date.

The `grizli` (grism redshift and line analysis) pipeline will serve as our primary workhorse for the reduction of the 3D-HST grism data (`https://github.com/gbrammer/grizli/`). This reduction will yield 1D and 2D spectra, emission-line maps, emission-line fluxes, and other quantities for each of these ∼400 galaxies in CANDELS. `grizli` works in a more sophisticated fashion than traditional data reduction methods of extraction of 1D spectra from standard slit spectroscopy, quantitatively modeling and fitting slitless spectroscopic data by overlapping spectra of objects in exposures taken with one or multiple grisms over multiple dispersion position angles. This process yields complete and uniform characterization of the suite of spectral line features of all objects observed in a given spectroscopic mode. The most relevant of these spectral properties for our analysis are redshifts, line fluxes, and emission-line maps. We have included Paβ in the default extractions of the `grizli` pipeline.

From these `grizli`-reduced data, we apply several selection criteria to build our Paβ

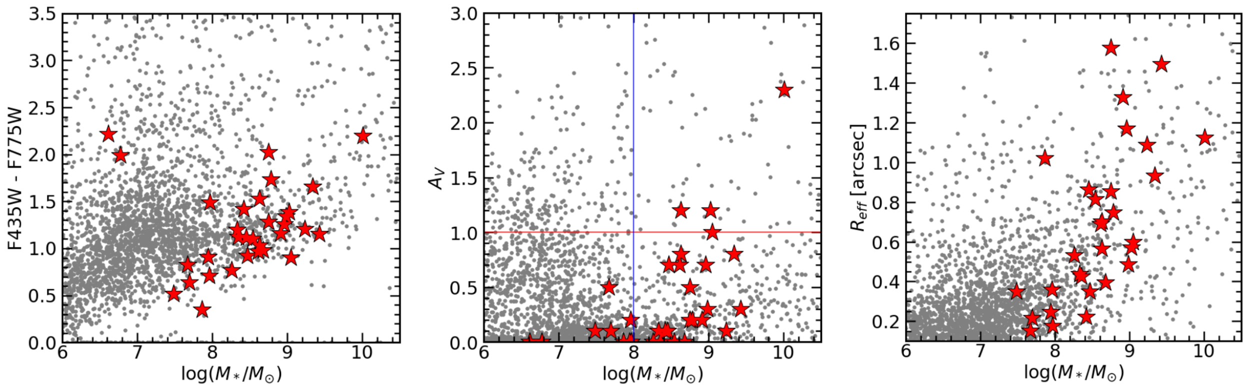

Figure 2: The color-mass (*left*), A_v-mass (*center*), and size-mass (*right*), relations for the CLEAR sample of Paβ-detected galaxies (red) and the full population of $z < 0.3$ galaxies in 3D-HST that form the parent sample of this proposal (gray). The CLEAR sample spans a wide range of rest-frame color, effective radius, and continuum attenuation profiles that is representative of the broader population of 3D-HST galaxies with $M_\star > 10^7 M_\odot$ in the same redshift range. In the center panel we show that Paβ SFRs are critically beneficial in highly dusty galaxies where UV/optical SFR tracers are severely attenuated (above $A_v = 1$, red line), and in low-mass galaxies without IR detections ($M_\star < 10^8\ M_\odot$, blue line). **The proposed sample of ∼400 Paβ-detected galaxies will enable studies of star formation rates and histories as a function of a representative range of galaxy properties.**

sample. For all objects in the redshift range $z < 0.3$, where Paβ is observable in the G141 spectrum, we will require the following: (1) The signal-to-noise ratio of Paβ flux to its error must be greater than 3. (2) The 2D spectra of each object must exist and be "good" by visual inspection, meaning there must be no obvious missing data or excessive contamination. We anticipate ∼400 objects in our sample after these cuts, based on the yield of 32 galaxies in the ∼12× smaller CLEAR study region.

We will use these data to measure Paβ star formation rates and histories for each of these ∼400 galaxies in all 3D-HST fields. The emission line fluxes will be extracted from the `grizli` analysis. We will compare Paβ luminosities to more commonly used SFR indicators, including attenuation corrected UV continuum and Hα luminosities, as shown in Figures 3 and 4. This analysis will give "gold standard" SFRs for each of these objects, in a sample a factor of several larger than all previous work.

We will also measure Paβ/Hα attenuation estimates for the ∼150 galaxies in our proposed sample with publicly available ground-based optical spectroscopy. Public spectra exist for the AEGIS (Cooper et al. 2011), COSMOS (Lilly et al. 2009), and GOODS-N (Wirth et al. 2004). (The GOODS-S and UDS fields have public *redshift* catalogs, but not compilations of spectra for Hα and Hβ flux measurements.) The ratio of Paβ/Hα offers a better estimate of interstellar dust attenuation than the most commonly used attenuation indicators, namely the Balmer decrement and ultraviolet continuum extinction.

Finally, we will also produce Paβ emission-line maps for ∼40 individual galaxies

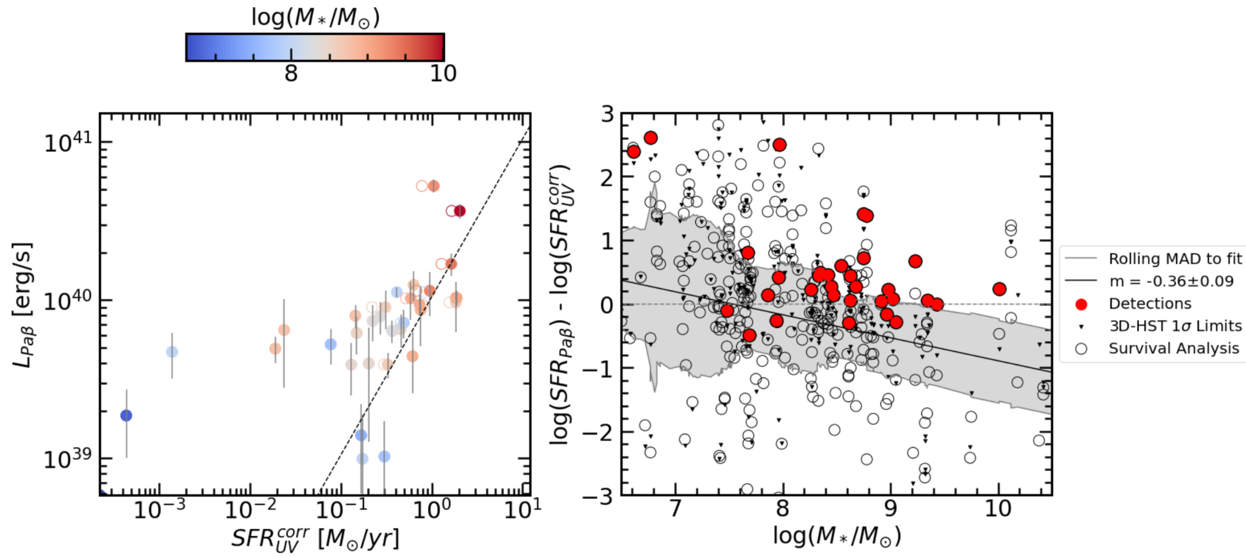

Figure 3: *Left:* The relation between Paβ luminosity and attenuation-corrected UV continuum SFR for galaxies in the CLEAR sample (solid points) and UV + IR SFR for those with well detected IR (hollow points). The grey line pictured is the Kennicutt-Schmidt SFR relation using the Paβ/Hα ratio for case B recombination at 10^4 K and a density of $N_e = 10^4$ cm^{-3}. *Right:* Survival analysis of the log ratio of Paβ and attenuation-corrected UV SFRs to stellar mass. The solid circles are the Paβ-detected objects in the CLEAR sample. Downward-facing black triangles represent the 1σ upper limits on all Paβ non-detections in CLEAR at $z < 0.3$, and open circles are randomly generated data from these non-detections using a half-normal distribution with standard deviation equal to the 1σ upper bounds. Linear regression fits for the full sample of detections and non-detections are shown (solid black line). The gray envelope shows rolling median absolute deviations of the sample and survival analysis points about the mean best fit line, respectively. The survival analysis particularly populates the lower-left of the plot where we cannot detect Paβ-emitting galaxies. Scatter of the Paβ/UV SFR ratio increases at lower stellar mass, indicating burstier star formation histories (Weisz et al. 2012, Guo et al. 2016). **The proposed sample will offer attenuation-insensitive Paβ star formation rates and histories for all ∼400 galaxies, and we will perform similar survival analyses to learn even more from the Paβ non-detections in 3D-HST.**

in this proposed sample. Emission-line maps will allow us to measure spatially resolved SFRs from the "gold standard" Paβ indicator. The CLEAR sample found good Paβ line maps through `grizli` for $\sim 10\%$ of galaxies in the sample, which we extend to our proposed sample to arrive at ∼40 galaxies for which we will derive Paβ emission-line maps. For the remainder of the 400 galaxies with fainter (SNR<10) Paβ detections, we will produce stacked Paβ maps in bins of galaxy mass and morphology (e.g. Nelson et al. 2016).

This work also benefits from measured and derived quantities from the exquisite CANDELS data in the 3D-HST pointings. In addition to the optical spectroscopy, the fields also include morphological information (Sérsic indices and effective radii) available from GAL-

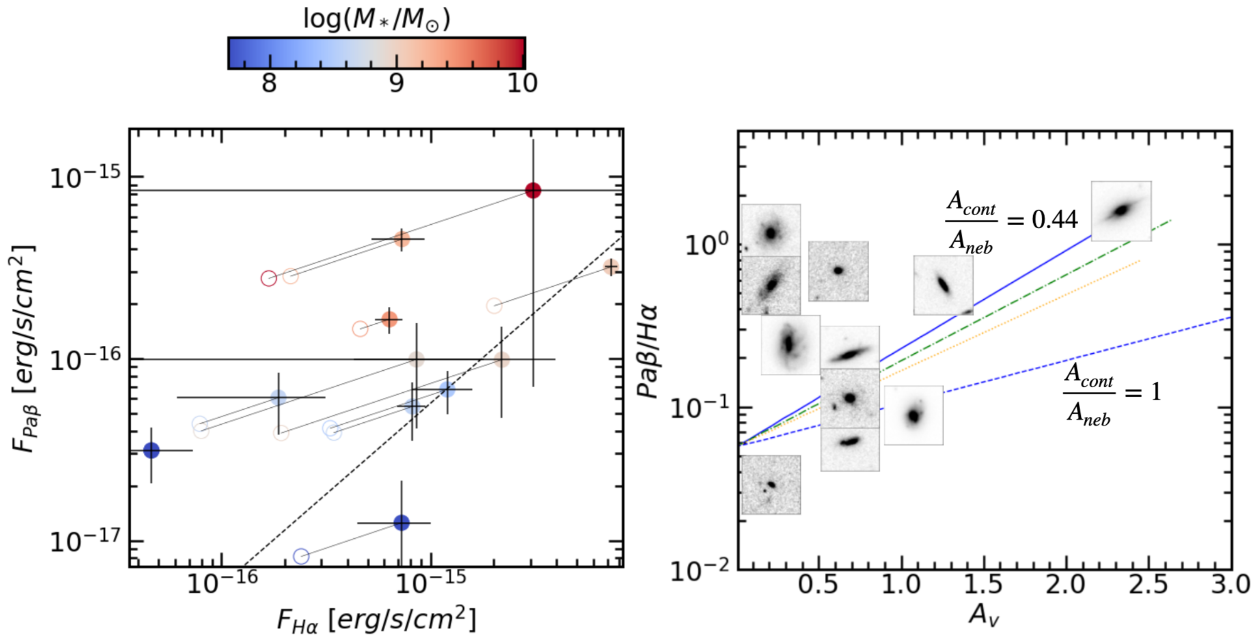

Figure 4: *Left:* Paβ and Hα fluxes for the 11 galaxies in our sample with TKRS optical spectroscopy, color coded by stellar mass. The gray line indicates Paβ/Hα = 1/17.6, appropriate for Case B recombination with $T = 10^4$ K and $n_e = 10^4$ cm^{-3} (Osterbrock 1989). Open circles show uncorrected fluxes and filled circles are dust-corrected fluxes, calculated using the observed Balmer decrement and a Calzetti et al. 2000 attenuation curve. About half of the sample has dust-corrected ratios of Paβ/Hα that is significantly larger than the expected ratio, over a wide range of stellar mass, UV slope, and Balmer decrement. This suggests the Balmer decrement dust corrections are frequently insufficient and a significant fraction of the Hα emission may be hidden in regions behind high optical depths that are seen in Paβ emission. *Right:* F125W direct images of the 11 galaxies in our sample with TKRS spectroscopy, overlaid on their log(Paβ/Hα) ratios and continuum A_V. Many of the galaxies with high Paβ/Hα ratios are edge-on disks, and the dustiest galaxy (in the upper right) has an apparent dust lane. **The proposed sample will offer superior Paβ/Hα dust attenuation estimates for ∼150 galaxies with matching optical spectroscopy.**

FIT (Peng et al. 2010, van der Wel et al. 2011), as well as UV continuum SFRs from the CANDELS/SHARDS multiwavelength catalog (Barro et al. 2019).

$\boxed{\textbf{Request Summary}}$ Matching the the scope of work outlined above, we anticipate requesting 1 year of graduate student salary, plus a half-month of summer salary for a faculty supervisor, travel funds, and page charges for one paper.

Timeline We propose a timeline for one year of graduate student-led projects as follows:

- Running `grizli` data reduction: ∼5 weeks
- Producing Paβ 1D and 2D spectra: ∼5 weeks
- Comparing Paβ emission to known SFR indicators (UV continuum and Hα) and performing survival analyses: ∼ 10 weeks
- Producing attenuation estimates from Paβ/Hα ratios: ∼5 weeks
- Time-allowing: Producing Paβ emission line maps from `grizli`: ∼5 weeks
- The remaining time (∼20 weeks) will be spent on a publication: *Paβ Star Formation Rates and Dust Attenuation in $z < 0.3$ 3D-HST Galaxies.*

References: • Alonso-Herrero, A., Rieke, G. H., Rieke, M. J., et al. 2006, ApJ,650, 835 • Barro, G., Pérez-González, P. G., Cava, A., et al. 2019, ApJS, 243,22 • Brammer, G. B., van Dokkum, P. G., & Coppi, P. 2008, ApJ, 686,1503 • Cleri, N. J., Trump, J. R., Backhaus, B. E., et al. 2020,arXiv e-prints, arXiv:2009.00617 • Cooper, M. C., Aird, J. A., Coil, A. L., et al. 2011, ApJS, 193, 14 • Estrada-Carpenter, V., Papovich, C., Momcheva, I., et al. 2019, ApJ,870, 133 • Grogin, N. A., Kocevski, D. D., Faber, S. M., et al. 2011, ApJS, 197,35 • Hinshaw, G., Larson, D., Komatsu, E., et al. 2013, ApJS, 208, 19 • Kennicutt, R. C., & Evans, N. J. 2012, ARA&A, 50, 531 • Koekemoer, A. M., Faber, S. M., Ferguson, H. C., et al. 2011, ApJS,197, 36 • Lilly, S. J., Le Brun, V., Maier, C., et al. 2009, ApJS, 184, 218 • Momcheva, I. G., Brammer, G. B., van Dokkum, P. G., et al. 2016,ApJS, 225, 27 • Osterbrock D. E. , 1989, Astrophysics of Gaseous Nebulae and Active Galactic Nuclei. Univ. Sci. Books, New York. • Peng, C. Y., Ho, L. C., Impey, C. D., & Rix, H.-W. 2010, AJ, 139,2097 • Sérsic, J. L. 1968, Atlas de Galaxias Australes • Skelton, R. E., Whitaker, K. E., Momcheva, I. G., et al. 2014, ApJS,214, 24 • van der Wel, A., Bell, E. F., Häussler, B., et al. 2012, ApJS, 203, 24 • Wirth, G. D., Willmer, C. N. A., Amico, P., et al. 2004, AJ, 127,3121 • Wuyts, S., Förster Schreiber, N. M., Lutz, D., et al. 2011, ApJ, 738,106